JOC The Journal of Organic Chemistry

Article

pubs.acs.org/joc

Theoretical Study on Cyclopropanation of *endo*-Dicyclopentadiene with Zinc Carbenoids: Effects of Solvent and $(ICH_2)_2Zn$

Ren Feng,[†] Ji-Jun Zou,*[,†] Xiangwen Zhang,[†] Li Wang,[†] and Haitao Zhao[‡]

[†]Key Laboratory for Green Chemical and Technology, School of Chemical Engineering and Technology, Tianjin University, Tianjin 300072, P. R. China

[‡]Department of Chemistry, School of Science, Tianjin University, Tianjin 300072, P. R. China

Supporting Information

ABSTRACT: A computational study using a hybrid DFT method (M06) on the cyclopropanation of *endo*-dicyclopentadiene with Simmons−Smith zinc carbenoids is reported. Each channel proceeds via the methylene-transfer mechanism with a reactant complex (RC) and subsquently a asynchronous transition state (TS). The channels with monomeric $IZnCH_2I$ attacking the double bonds from the exo-face have a much lower barrier (about 16.17−18.43 kcal/mol) in the gas phase, compared with the channels from the endo-face (21.80−31.13 kcal/mol). Thus, P1 and P3 are the primary cyclopropanated compounds, and P5 is the sole final product, representing remarkable stereospecificity. When considering the bulk solvent effect of diethyl ether, the barriers are decreased about 0.50−7.77 kcal/mol due to more "destabilization"of RC than TS. The solvated $(ICH_2)_2Zn$ can further reduce the barriers about 0.18−2.30 kcal/mol. In addition, the solvated $IZnCH_2I$ and $(ICH_2)_2Zn$ do not change the reaction pathways and retain the stereospecificity. Our computational results agree with the experimental observations quite well and suggest that both $IZnCH_2I$ and $(ICH_2)_2Zn$ might be the active species in the real reaction system. Regarding the solvent effect, the polar continuum model is more realistic than the direct involvement of diethyl ether molecules.

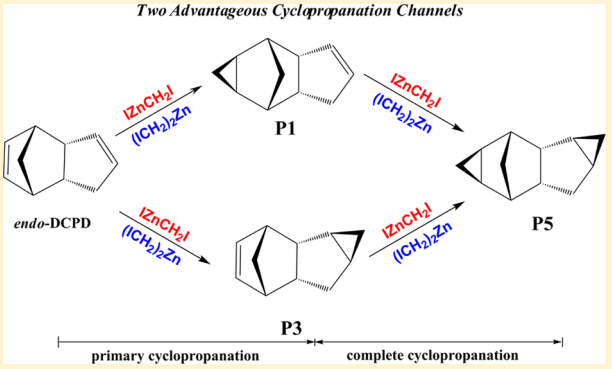

INTRODUCTION

In 1958, Simmons and Smith reported a synthesis strategy for cyclopropanated compounds involving the reaction of cyclohexene with iodomethylzinc iodide.[1,2] Subseqently, they treated *endo*-dicyclopentadiene (*endo*-DCPD) with methylene iodide and an equivalent amount of zinc−copper couple in refluxing ether and obtained a single saturated product of pentacyclo-[6.3.1.$0^{2,7}$.$0^{3,5}$.$0^{9,11}$]dodecane (P5, 63%) and two isomeric cycloolefins $C_{11}H_{14}$ (P1, 12%; P3, 11%), along with unreacted starting materials (14%) (see Scheme 1).[3] Since that report, the efficacious and facile Simmons−Smith reaction has been widely employed to prepare various cylcopropanated compounds.[4−11] To explain the reaction, Simmons and Smith proposed a methylene-transfer mechnism with a concerted [1 + 2] addition via a butterfly-type transition state, accompanied by the migration of halide from carbon to metal atom.[2] Later, a two-step carbometalation mechanism involving a four-centered transition state was also postulated (see Scheme 2).[12−14] The presence of mechanistic dichotomy inspired many theoretical studies. Bernardi used DFT method to investigate the reaction between $ClCH_2ZnCl$ and ethene and found that the concerted methylene-transfer channel has a lower barrier with respect to the insertion channel.[15] Nakamura reported that methlyene-transfer represents the reaction reality for the cylcopropanation of ethene with $LiCH_2Cl$ or $ClZnCH_2Cl$.[13,14] Recent calculations also suggest that the methylene-transfer pathway is dominant in cyclopropanation using aluminum carbenoids.[16−18] Furthermore, some researchers elucidated the influence of carbenoid structure on the cyclopropanation. Zhao reported that geminal dizinc carbenoids $(RZn)_2CHI$ (R = Et or I) can substantially lower the reaction barrier, compared with monomeric zinc carbenoids.[19] Hermann and Boche elaborated the influence of leaving group X (X = F, Cl, Br, I, OH) on the nature of $XZnCH_2X$ carbenoids and concluded that $IZnCH_2I$ has the lowest barrier.[20] Also, samarium carbenoids are reported to show properties similar to those of lithium carbenoids.[21,22]

Scheme 1. Experimental Results from the Cyclopropanation of *endo*-DCPD with Zinc Carbenoids in Diethyl Ether Solvent

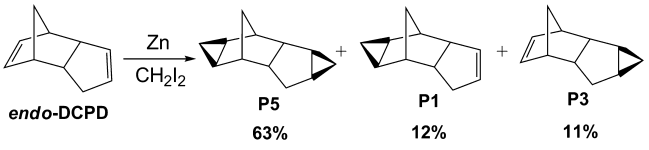

Received: July 23, 2012
Published: October 22, 2012

Scheme 2. Methylene-Transfer and Carbometalation Mechanisms for Cyclopropanation with Carbenoids

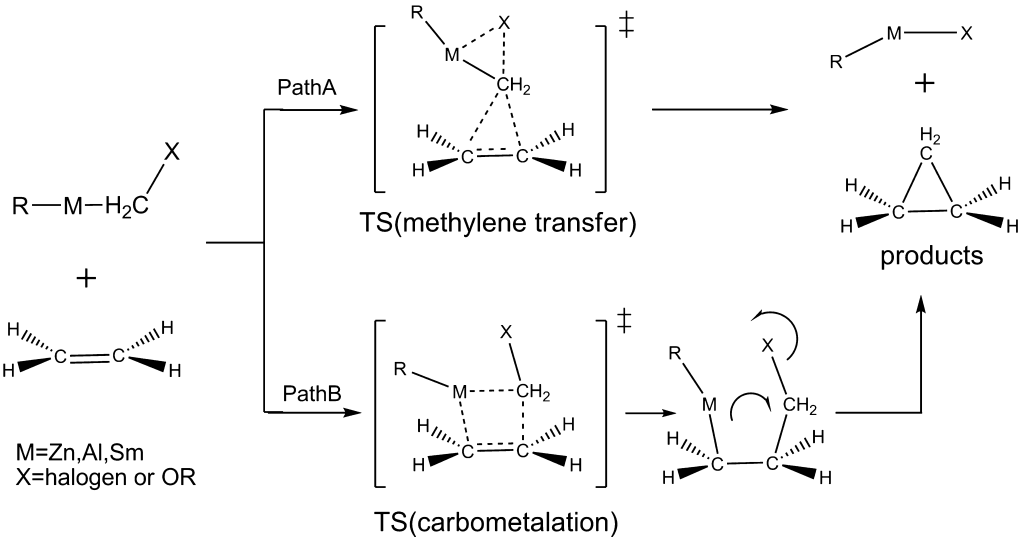

Scheme 3. Anticipated Cyclopropanated Compounds of *endo*-DCPD with Zinc Carbenoids

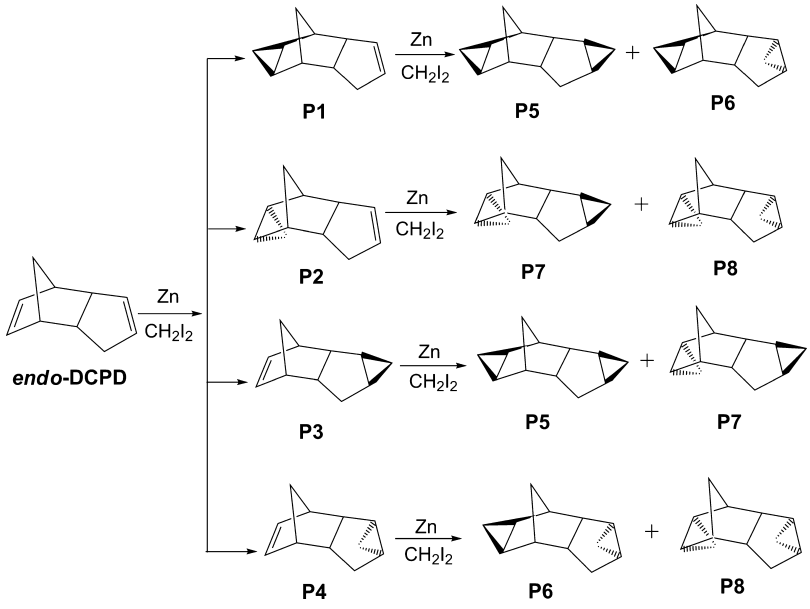

Meanwhile, under real conditions, cylcopropanation reactions are usually conducted in oxygen-containing solvents.[23] The solvent effect might be very significant not only on the structure of the carbenoid but also on the reaction barrier.[24] For example, *n*-BuLi itself is a hexamer (n-Bu_6Li_6) in the solid state. However, in polar solvents such as diethyl ether, tetramers and dimers of *n*-BuLi become predominant.[25] The calculation implemented by Lawrence showed that dimers, trimers, and even tetramers may coexist in THF solution, along with free lithium carbenoids.[26] Ke and co-workers illustrated that the aggregation of lithum carbenoids enhances the methylene-transfer pathway.[27] For zinc carbenoids, Simmons and Rickborn reached the same conclusion that a mixture of $IZnCH_2I$ and $(ICH_2)_2Zn$ is formed as a result of Schelenk-type equilibrium in diethyl ether.[23,28] Then, Fabisch and Mitchell experimentally detected $(ICH_2)_2Zn$ by NMR, but it is not clear whether these carbenoids can promote the cyclopropanation reaction.[29]

On the other hand, most of the previous theoretical studies are confined to the cyclopropanation of simple and symmetrical olefins such as ethene, whereas the cyclopropanation mechanism of multicyclic olefins such as *endo*-DCPD were insufficiently investigated. The low symmetry of *endo*-DCPD with two double bonds makes the reaction channel more complicated, which is different from that of simple alkenes. Moreover, the cyclopropanation of *endo*-DCPD is very attractive in the synthesis of advanced aerospace fuel[30] due to its high density and energy.[31−33] In this work, we carried out a computational study on the cyclopropanation of *endo*-DCPD with zinc carbenoids using a hybrid DFT method (M06), focusing on the effects of diethyl ether solvent and $(ICH_2)_2Zn$.

■ COMPUTATIONAL DETAILS

All the stationary molecules and transtition states were fully optimized with hybrid density functional M06.[34,35] The 6-311+G(d,p) basis set was implemented for C, H, Zn, and O atoms, and the LANL2DZ basis set[36−38] was used for the I atom. The combined basis set was

dx.doi.org/10.1021/jo3015616 | J. Org. Chem. 2012, 77, 10065−10072

abbreviated to BS in the following discussion. Analytical frequency calculations at the same level were performed to confirm the optimized stuctures as either a minimum or a first-order saddle point, as well as to obtain the sum of electronic and zero-point energy. Intrinsic reaction coordinate (IRC) calculations[39,40] at the same level were performed to confirm that the optimized transition states correctly connect their corresponding reactants and products. Natural bond orbital (NBO) analysis[41,42] was performed to check the charge distributions of related atoms. All the calculations were carried out in the Gaussian 09 package.[43] If not mentioned, the solvent-corrected geometries and energies were calculated with the self-cosistent reaction field (SCRF) method (polar continuum model).[44,45]

RESULTS AND DISCUSSION

1. Cyclopropanation of *endo*-DCPD with Monomeric $IZnCH_2I$ in the Gas Phase. As mentioned in the introduction, the methylene-transfer mechiansm is more favorable in the cyclopropanation reaction, so only this mechiansm was considered in this work. The carbenoid can attack both C=C bonds in norbornyl and cyclopentyl rings (denoted as NB and CP, respectively) from different directions, and various primary and complete cyclopropanated compounds can be expected (see Scheme 3).

a. Primary Cyclopropanation of endo-DCPD. The optimized structures and calculated energies of starting materials (SM), reaction complexes (RC), transition states (TS), and product complexes (PC) with ZPE correction on the primary cyclopropanation of *endo*-DCPD to form P1−P4 in the gas phase are displayed in Figure 1. The most stable monomeric $IZnCH_2I$ in the gas phase possesses a special geometry structure with I^1, Zn, I^2, and C^1 planar (the I^2−C^1−Zn−I^1 dihedral angle is −0.246°), and the length of C^1−I^2, C^1−Zn, and Zn−I^1 is 2.183, 1.932, and 2.429 Å, respectively. The Zn−C^1−I^2, I^2−C^1−H, Zn−C^1−H, and H−C^1−H angles are 105.3°, 106.1°, 114.3°, and 109.7°, respectively (see Figure 3), which indicates that the carbon atom in the monomeric zinc carbenoid is almost sp^3 hybridized. This is very distinct from the almost sp^2 hybridization in $LiCH_2I$ and $ISmCH_2I$.[14,21] As the zinc carbenoid approaches the NB C=C bond, the interaction between the zinc vacant p orbital and C=C π orbital promotes the formation of π-type complexes (RC1, RC2). The NBO calculations reveal that natural charges of Zn decrease from 0.871 in isolated $IZnCH_2I$ to 0.854, 0.815 in RC1, RC2, respectively, and the C^1 charges decrease respectively from −1.155 to −1.168, −1.182. This reflects the increment of the electron density of C^1 and Zn in π-type complexes, which stabilizes the π-type complexes and significantly reduces the energy of reactants by 8.00 and 11.92 kcal/mol, respectively (see Figure 1). Subsequently, the two complexes evolve into transition states (TS1, TS2) that have the energy of 10.43 and 19.21 kcal/mol, respectively. Then the cleavage of C^1−I^2 and C^1−Zn leads to the formation of C^1−C^3 and C^1−C^2 bonds.

As RC1 (RC2) goes to TS1 (TS2), the π electrons shift from the C^2=C^3 π orbital to C^1−I^2 σ* orbital, pushing the electrons in the C^1−I^2 σ orbital to the I^2 atom. In approaching the TS, the electrons from the C^1−I^2 σ-bond facilitate the formation of a Zn−I^2 bond. Furthermore, this electron transfer contributes to the partial formation of C^1−C^2, C^1−C^3 and the partial breaking of C^1−I^2. The length of the C^1−C^2 bond is slightly different from that of the C^1−C^3 bond in both TSs, reflecting asynchronous addition of methylene to the C=C bond. This result is in agreement with the reports that monomeric Ti, Zn, Al, Sm, and Li carbenoids with low symmetry react with

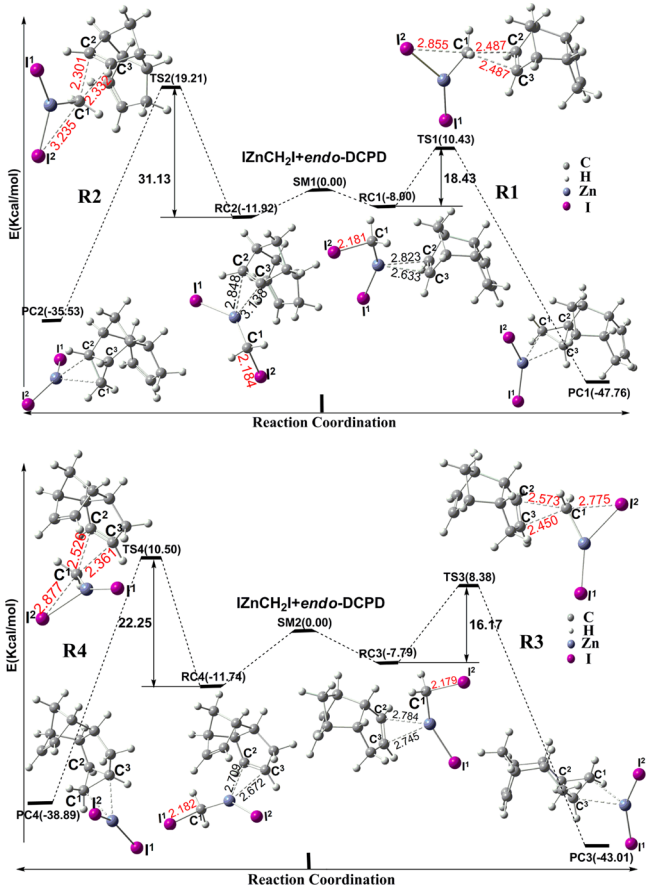

Figure 1. The reaction profiles of the primary cyclopropanation of the NB (R1, R2) and CP (R3, R4) C=C bond of *endo*-DCPD with monomeric $IZnCH_2I$ (M06/BS level) in the gas phase. The bond lengths are given in angstroms. Energies relative to the starting materials are shown in the parentheses.

ethylene in an asynchronous manner.[17−19,27] Furthermore, the planar ethylene moiety undergoes significant pyramidalization (5.57° and 21.25° for C^2, 4.71° and 19.85° for C^3 in TS1 and TS2, respectively), which demonstrates that the sp^2→sp^3 rehybridization of C^2 and C^3 is required for the formation of the cyclopropane ring.

The reactions on the CP C=C bond are similar to those on the NB C=C bond (see Figure 1). The energy of the reactant complexes (RC3, RC4) is 7.79 and 11.75 kcal/mol lower than that of SM2, respectively. In TS3 and TS4, the C^1−C^2 bond is longer than the corresponding C^1−C^3 bond, which is also significant evidence for asynchronous addition on the CP C=C bond.

The calculated barrier for R1 and R3 (18.43 and 16.17 kcal/mol) is much lower than that for R2 and R4 (31.13 and 22.25 kcal/mol), respectively (see Figure 1), demonstrating that $IZnCH_2I$ tends to approach the double bond from the exo-face. After the TS geometries are carefully checked, it is found that the access from the endo-face (R2, R4) leads the C=C bond to undergo considerable pyramidalization (21.25° and 7.33° for C^2, 19.85° and 10.18° for C^3, respectively). Meanwhile the pyramidalization with exo-access (R1, R3) is much smaller (5.57° and 2.4° for C^2, 4.71° and 6.32° for C^3, respectively). As a result, the RC→TS evolution with the access from the endo-face has to overcome higher energy barrier. In addition, the energy gap between the frontier orbitals (LUMO and HOMO)

dx.doi.org/10.1021/jo3015616 | J. Org. Chem. 2012, 77, 10065−10072

(see Table 1) of P1 and P3 is, respectively, 0.006 and 0.008 au higher than that of P2 and P4, which suggests that P1 and P3

Table 1. Energy Gaps (au) between the LUMOs and HOMOs of P1−P7 Computed at the M06/BS Level

	in gas phase			in diethyl ether		
	LUMO	HOMO	E_g	LUMO	HOMO	E_g
P1	−0.028	−0.252	0.224	−0.027	−0.253	0.226
P2	−0.030	−0.248	0.218	−0.030	−0.248	0.218
P3	−0.028	−0.253	0.225	−0.027	−0.254	0.227
P4	−0.030	−0.247	0.217	−0.029	−0.247	0.218
P5	−0.028	−0.267	0.239	−0.027	−0.267	0.240
P6	−0.029	−0.263	0.234	−0.028	−0.263	0.235
P7	−0.030	−0.266	0.236	−0.029	−0.267	0.238

[a] E_g = LUMO − HOMO

are more stable. The thermodynamically favorable products (P1 and P3) predict the stereospecificity of cyclopropanation. Actually, P1 and P3 appear in amounts equal to those of the primary compounds in the experiment.[3] Thus, in the following section, only the further cyclopropanation of P1 and P3 are considered.

b. Complete Cyclopropanation of P1 and P3. As shown in Figure 2, when monomeric $IZnCH_2I$ approaches the remaining double bond in P1 and P3, π-type complexes (RC5−RC8) are

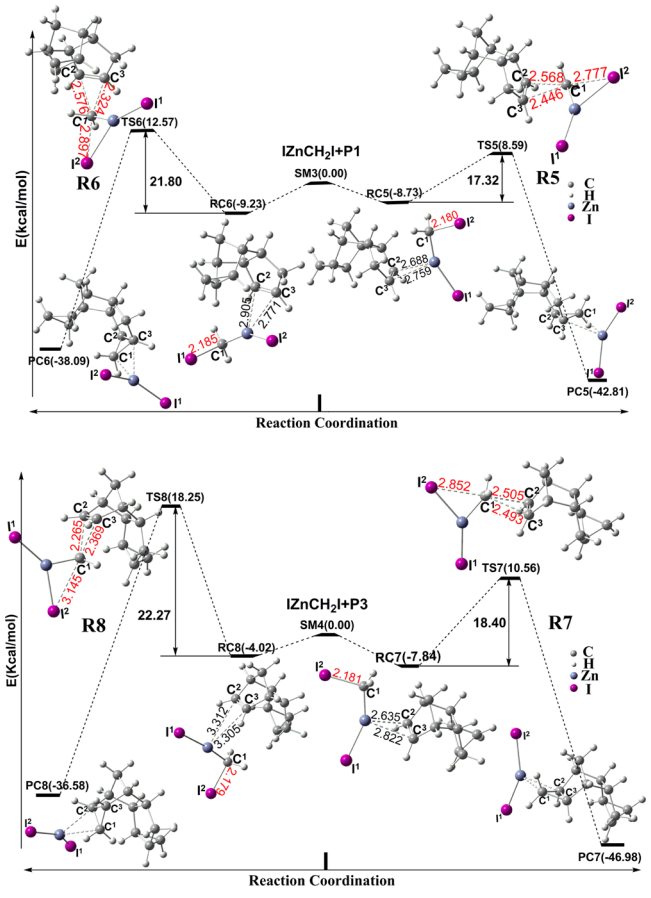

Figure 2. The reaction profiles of the complete cyclopropanation of P1 (R5, R6) and P3 (R7, R8) with the monomeric $IZnCH_2I$ in the gas phase (M06/BS level). The bond lengths are given in angstroms. Energies relative to the starting materials are shown in the parentheses.

formed with the energy of reaction systems lowered. Then the reactions go from RCs to TSs by overcoming the energy barrier. The discrepancy in bond length of C^1-C^3 and C^1-C^2 in TS5−TS8 also reveals the asynchronous addition to the double bond. Note that the structural changes from RC to the corresponding TS can reflect the order of the reaction barrier. The elongation of the C^1-I^2 bond in TS6 is 0.115 Å longer than that in TS5, so the barrier of R6 is higher (4.48 kcal/mol) than that of R5. Similarly, the elongation of the C^1-I^2 bond in TS8 is 0.295 Å longer than that in TS7, so R8 has a barrier 3.87 kcal/mol higher than that of R7 (see Figure 2).

The calculated barriers (see Figure 2) show that R5 and R7 are more facile to occur while R6 and R8 are not, which implies that the monomeric $IZnCH_2I$ still tends to attack the remaining C═C bond from the exo-face. The two channels both lead to the stereospecific final product P5, in agreement with experimental results.[3] In fact, P5 (0.239 au) has the highest LUMO−HOMO energy gap among all the possible complete cyclopropanated products (see Table 1).

2. Cyclopropanation of *endo*-DCPD with Monomeric $IZnCH_2I$ in Diethyl Ether Solvent. The bulk solvent effect on the cyclopropanation with monomeric $IZnCH_2I$ was investigated using the PCM solvation. Although the direct involvement of solvent molecules is possible, the result indicates that the former is more realistic (see below). Diethyl ether solvent does not significantly change the structures of solvated monomeric $IZnCH_2I$ (see Figure 3) and transition

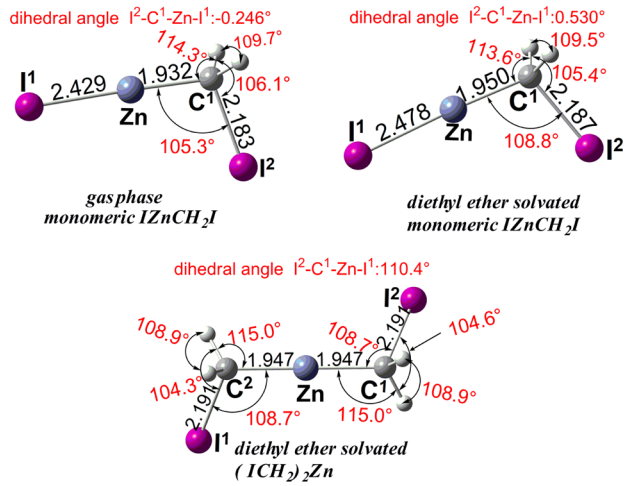

Figure 3. The geometries of zinc carbenoids involved in this study computed at the M06/BS level. The bond lengths are given in angstroms.

states (TS1′−TS8′) (see Figure 4). The C^1-Zn, C^1-I^2, and $Zn-I^1$ bond lengths of solvated $IZnCH_2I$ are just slightly elongated by 0.018, 0.004, and 0.049 Å and the I^2-C^1-H, $Zn-C^1-H$, and $H-C^1-H$ angles are 0.7°, 0.7°, and 0.2° smaller than that in the gas phase, respectively. I^1, Zn, C^1, and I^2 are still planar because the $I^2-C^1-Zn-I^1$ dihedral angle is 0.530°. For TS1′−TS8′, the difference between the length of the C^1-C^2 and C^1-C^3 bonds confirms the asynchronous behavior of solvated monomeric $IZnCH_2I$.

Although the absolute energies are lower than in the case of the gas phase, both RCs and TSs are "destabilized" in diethyl ether solvent because their energies relative to the starting materials(SM) are raised to some degree (see Table 2). Furthermore, the "destabilization" is more obvious for the RCs,

dx.doi.org/10.1021/jo3015616 | J. Org. Chem. 2012, 77, 10065−10072

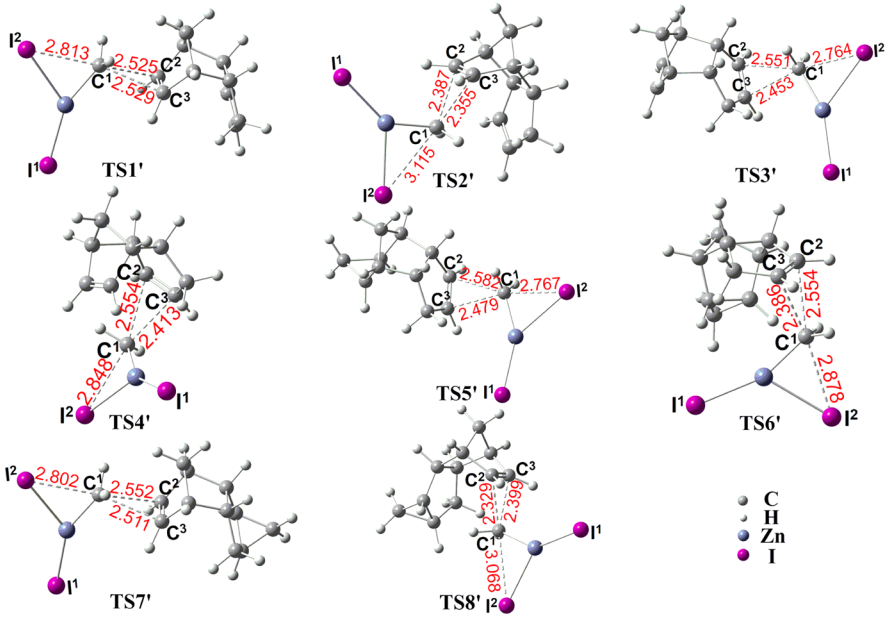

Figure 4. The geometries of the transition state of the cyclopropanation with monomeric $IZnCH_2I$ in diethyl ether solvent computed at the M06/BS level. The bond lengths are given in angstroms.

Table 2. Relative Energies (kcal/mol) of Reactant Complexes, Transition States, and Barriers for the Reaction Channels in Diethyl Ether Solvent Computed at the M06/BS Level

reaction channels[a]	E (RC)	E (TS)	ΔE (barrier)
R1′	−4.19	12.95	17.14
R2′	−2.06	21.30	23.35
R3′	−4.07	11.60	15.68
R4′	−5.76	14.00	19.77
R5′	−3.84	11.78	15.62
R6′	−3.94	15.73	19.67
R7′	−4.10	13.00	17.10
R8′	−2.53	20.32	22.85
R1″	−5.20	10.26	15.47
R2″	−5.54	18.39	23.93
R3″	−4.10	9.27	13.37
R4″	−6.96	12.95	19.91
R5″	−3.83	10.09	13.92
R6″	−4.92	14.57	19.49
R7″	−5.60	9.93	15.53
R8″	−6.09	17.42	23.51

[a]R1′−R8′ represent the channels with monomeric $IZnCH_2I$ in diethyl ether solvent. R1″−R8″ represent the channels with $(ICH_2)_2Zn$ in diethyl ether solvent.

so the barriers decrease compared with the cases in the gas phase. For example, the total energy of RC1′ is 3.81 kcal/mol higher than that of RC1 while TS1′ is just 2.52 kcal/mol higher than TS1; therefore, the barrier of R1′ decreases from 18.43 kcal/mol in the gas phase to 17.14 kcal/mol in solvent.

Additionally, NBO analysis reveals that the C^1 and Zn natural charges of RC1′−RC8′ are more positive compared with those of RC1−RC8 (see Table 3). For example, the natural charges of C^1 increase from −1.179 in RC1 to −1.168 in RC1′, and the Zn natural charges rise from 0.854 to 0.949. The increment of C^1 and Zn charges suggests the enhanced electrophilicity of $IZnCH_2I$ in solvated reactant complexes, which also contributes to the improved reactivity in cyclopropanation.

Table 3. Natural Charges of C^1 and Zn in Reactant Complexes Computed at the M06/BS Level

	in gas phase (RC)		in diethyl ether (RC′)		$(ICH_2)_2Zn$ in diethyl ether (RC″)	
reaction channels	C^1	Zn	C^1	Zn	C^1	Zn
1	−1.179	0.854	−1.168	0.949	−1.160	1.194
2	−1.168	0.815	−1.160	1.011	−1.161	1.217
3	−1.182	0.856	−1.172	0.964	−1.158	1.238
4	−1.176	0.819	−1.167	0.895	−1.163	1.218
5	−1.176	0.854	−1.168	0.974	−1.157	1.241
6	−1.168	0.810	−1.169	0.868	−1.165	1.224
7	−1.179	0.857	−1.169	0.960	−1.158	1.192
8	−1.169	0.844	−1.168	1.023	−1.165	1.224

As illustrated in Table 2, the barriers for $IZnCH_2I$ attacking from the exo-face (R1′, R3′, R5′, R7′) are much lower than that of their competitive channels from the endo-face (R2′, R4′, R6′, R8′), predicting that the reaction in solvent still shows stereospecificity. The energy gap between the frontier orbitals (see Table 1) of P1, P3, and P5 is, respectively, 0.008, 0.009, and 0.005 au higher than that of P2, P4, and P6 in solvent. As a result, P1 and P3 are the primary cyclopropanated compounds, and P5 is the sole final product, in agreement with experimental results.[3]

The direct involvement of diethyl ether solvent was also assessed by considering the monomeric $IZnCH_2I$ coordinated with one diethyl ether molecule. Two reaction channels ($R1^C$, $R3^C$) with coordinated $IZnCH_2I$ attacking NB and CP C═C bonds from the exo-face were probed. As shown in Figure 5, in the TSs ($TS1^C$, $TS3^C$), the Zn atom is coordinated by the O atom of diethyl ether with a Zn−O bond of 2.143 and 2.142 Å, respectively. Although the lengths of C^1−I^2, C^1−C^2, and C^1−C^3 in $TS1^C$ and $TS3^C$ are almost the same as those in TS1′ and TS3′, the C^1−I^2−Zn−C^1 dihedral angle in $TS1^C$ and $TS3^C$ (−140.7° and −137.8°, respectively) is much different from that in TS1′ and TS3′ (both 180°). This indicates that the

dx.doi.org/10.1021/jo3015616 | J. Org. Chem. 2012, 77, 10065−10072

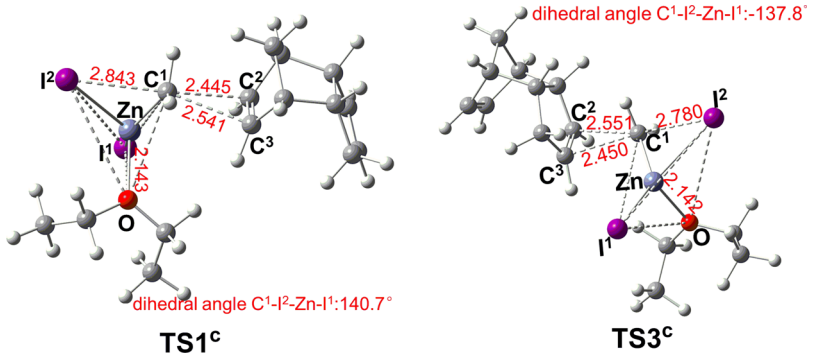

Figure 5. The geometries of the transition state of the cyclopropanation with monomeric $IZnCH_2I$ coordinated with one diethyl ether molecule computed at the M06/BS level. The bond lengths are given in angstroms.

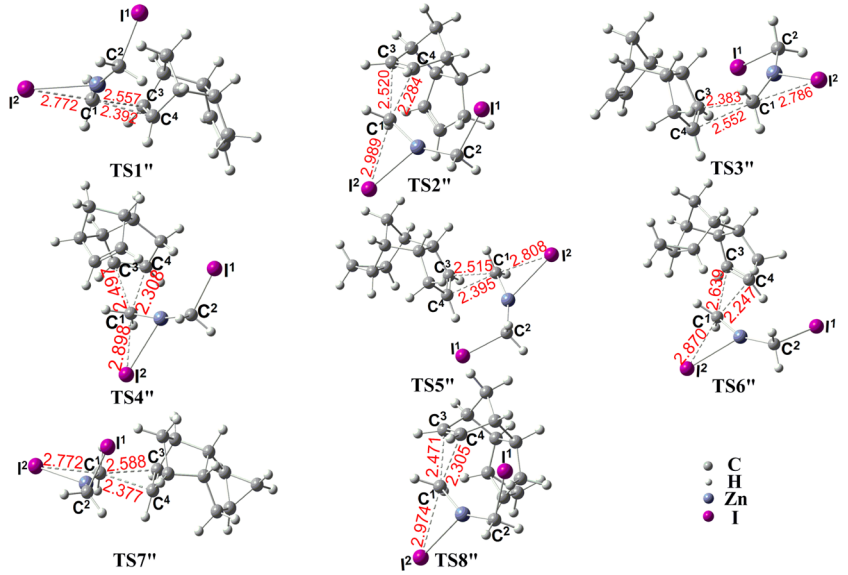

Figure 6. The geometries of the transition state of cyclopropanation with $(ICH_2)_2Zn$ in the diethyl ether solvent computed at the M06/BS level. The bond lengths are given in angstroms.

planar monomeric $IZnCH_2I$ is transformed into pyramidal geometry when one diethyl ether molecule coordinates a Zn atom, due to the strong electronic repulsion between O and the two iodine atoms.

Compared with the PCM solvation (see Table 3), the electrophilicity increase for coordinated monomeric $IZnCH_2I$ in the π-complexes ($RC1^C$ and $RC3^C$) is not so much. The natural charge of C^1 is −1.182 and −1.189 in $RC1^C$ and $RC3^C$, and the Zn charge is 0.887 and 0.897, respectively. As a result, the barrier of $R1^C$ and $R3^C$ (17.90 and 15.82 kcal/mol) is slight higher than that of R1′ and R3′ (17.14 and 15.68 kcal/mol), respectively. This result indicates that the direct involvement of the solvent molecule is less possible than the PCM solvation.

3. Cyclopropanation of *endo*-DCPD with $(ICH_2)_2Zn$ in Diethyl Ether Solvent. Theoretical and experimental research studies have shown that $(ICH_2)_2Zn$ will be formed in diethyl ether solvent via Schelenk-type equilibrium,[23,28,29] but it is not clear whether this carbenoid plays a role in the cyclopropanation reaction. As displayed in Figure 3, the dihedral angle $I^2-C^1-Zn-I^1$ in solvated $(ICH_2)_2Zn$ is 110.4°, predicting that the I^2 and I^1 are not planar. This is very distinct from the monomeric $IZnCH_2I$ in the gas phase and solvent. In this structure, the distance between the two iodine atoms is maximized, so that the electrostatic repulsion and steric hindrance are the lowest, resulting in the highest stability among all possible conformations. In contrast, the $Zn-C^{1(2)}-H$, $H-C^{1(2)}-H$, $I^2-C^{1(2)}-H$, and $Zn-C^{1(2)}-I^2$ angles in $(ICH_2)_2Zn$ are almost identical to those in solvated monomeric $IZnCH_2I$, which suggests that C^1 and C^2 in $(ICH_2)_2Zn$ are also sp^3 hybridized. Furthermore, the length of C^2-Zn and C^2-I^1 is identical to that of C^1-Zn and C^1-I^2, respectively, so that both methylene moieties in $(ICH_2)_2Zn$ can react with the C=C bond of *endo*-DCPD. The difference between the C^1-C^3 bond and C^1-C^2 bond in TS1′−TS8″ (see Figure 6) means that $(ICH_2)_2Zn$ also accesses the NB and CP C=C bonds in an asynchronous manner.

Similar to the cyclopropanation with monomeric $IZnCH_2I$, the reaction with $(ICH_2)_2Zn$ also proceeds via a butterfly-type TS (see Figure 6). The C^1 atom on one of the methylene moieties partially bonds with C^3 and C^4, forming a rudimental cyclopropane ring. The C^1-I^2 bond is simultaneously elongated into partial fragmentation, and finally this bond is completely broken with the electron-rich I^2 atom attaching to the Zn atom. Unlike the reaction with $IZnCH_2I$, the byproduct is $IZnCH_2I$ instead of ZnI_2, which can participate in the formation of $(ICH_2)_2Zn$ again.

Notably, the involvement of $(ICH_2)_2Zn$ can decrease the barriers (0.18−2.30 kcal/mol) of most reaction channels,

dx.doi.org/10.1021/jo3015616 | J. Org. Chem. 2012, 77, 10065−10072

compared with the case of monomeric $IZnCH_2I$ in solvent (see Table 2). The barriers of R1″, R3″, R5″, R7″ are much lower than their competitive reactions (R2″, R4″, R6″, R8″). That is, $(ICH_2)_2Zn$ facilitates the reactions and retains the stereospecificity. The natural charges of C^1 and Zn atom in most of RC″ are increased when compared with those in the corresponding RC′ (see Table 3), indicating the further enhanced electrophilicity of $(ICH_2)_2Zn$ in RC″.[21] Taking reaction channel 1 as an example, the natural charges of C^1 increase from −1.168 in RC1′ to −1.160 in RC1″ and the Zn natural charges rise from 0.949 to 1.194. The increase in electrophilic character of $(ICH_2)_2Zn$ in RC″ is believed to contribute to the high reactivity. This result shows that the reaction channels with $(ICH_2)_2Zn$ are more preferred than those with monomeric $IZnCH_2I$. Therefore, in the real solvated system, the active carbenoids might be a mixture of monomeric $IZnCH_2I$ and $(ICH_2)_2Zn$. However, it is difficult to determine which one contributes more to the reaction at the present stage.

CONCLUSION

The cyclopropanation of *endo*-dicyclopentadiene occurs via a π-complex and succeeding an asynchronous transition state. The carbenoids tend to attack the C═C bonds from the exo-face and show lower barriers, compared with channels from the endo-face. Thus, a high stereospecificity is obtained. Diethyl ether solvent notably decreases the reaction barriers because of more "destabilization" of reactant complexes (RC′) than of transition states (TS′). The PCM solvation is more realistic than the direct involvement of solvent molecules. Moreover, when solvated $(ICH_2)_2Zn$ is involved, the reaction barriers are further decreased, so it is very possible that the mixture of $IZnCH_2I$ and $(ICH_2)_2Zn$ serves as the active carbenoids in reality. In all the calculations (in the gas phase or solvent, $IZnCH_2I$ and $(ICH_2)_2Zn$ carbenoids), P1 and P3 are the primary cyclopropanated products and P5 is the sole final product, in good agreement with the experimental results.

ASSOCIATED CONTENT

Supporting Information

The geometry structures, Cartesian coordinates, and the absolute electronic energies with zero-point correction for the species involved in our study. This material is available free of charge via the Internet at http://pubs.acs.org.

AUTHOR INFORMATION

Corresponding Author

*E-mail: jj_zou@tju.edu.cn.

Notes

The authors declare no competing financial interest.

ACKNOWLEDGMENTS

The authors appreciate the support from the Natural Science Foundation of China (21222607, 20906069), the Foundation for the Author of National Excellent Doctoral Dissertation of China (200955), and the Program for New Century Excellent Talents in University (NCET-09-0594).

REFERENCES

(1) Simmons, H. E.; Smith, R. D. *J. Am. Chem. Soc.* **1958**, *80*, 5323−5324.
(2) Simmons, H. E.; Smith, R. D. *J. Am. Chem. Soc.* **1959**, *81*, 4256−4264.
(3) Simmons, H. E.; Blanchard, E. P.; Smith, R. D. *J. Am. Chem. Soc.* **1964**, *86*, 1347−1356.
(4) Lautens, M.; Klute, W.; Tam, W. *Chem. Rev.* **1996**, *96*, 49−92.
(5) DelMonte, A. J.; Dowdy, E. D.; Watson, D. J. *Topics in Organometallic Chemistry*; Springer, Inc.: Heidelberg, 2004,; Vol. *6*, pp 97−122.
(6) Boche, G.; Lohrenz, J. C. W. *Chem. Rev.* **2001**, *101*, 697−756.
(7) Lebel, H.; Marcoux, J.-F.; Molinaro, C.; Charette, A. B. *Chem. Rev.* **2003**, *103*, 977−1050.
(8) Long, J.; Yuan, Y.; Shi, Y. *J. Am. Chem. Soc.* **2003**, *125*, 13632−13633.
(9) Lorenz, J. C.; Long, J.; Yang, Z.; Xue, S.; Xie, Y.; Shi, Y. *J. Am. Chem. Soc.* **2003**, *69*, 327−334.
(10) Cousins, G. S.; Hoberg, J. O. *Chem. Soc. Rev.* **2000**, *29*, 165−174.
(11) Charette, A. B.; Marcoux, J. F. *Synlett* **1995**, 1197−1207.
(12) Stiasny, H. C.; Hoffmann, R. W. *Chem.—Eur. J.* **1995**, *1*, 619−624.
(13) Hirai, A.; Nakamura, M.; Nakamura, E. *Chem. Lett.* **1998**, 927−928.
(14) Nakamura, M.; Hirai, A.; Nakamura, E. *J. Am. Chem. Soc.* **2003**, *125*, 2341−2350.
(15) Bernardi, F.; Bottoni, A.; Miscione, G. P. *J. Am. Chem. Soc.* **1997**, *119*, 12300−12305.
(16) Li, Z.-H; He, L.-Z; Teng, G.-Y. *Arabian J. Chem.* **2011**, *4*, 379−382.
(17) Zhuang, S.-X.; Zhang, X.-H. *J. Mol. Struct.: THEOCHEM* **2009**, *894*, 14−19.
(18) Li, Z.-H.; Ke, Z.; Zhao, C.; Geng, Z.-Y.; Wang, Y,-C.; Phillips, D. L. *Organometallics* **2006**, *25*, 3735−3742.
(19) Zhao, C.; Wang, D.; Phillips, D. L. *J. Am. Chem. Soc.* **2002**, *124*, 12903−12914.
(20) Hermann, H.; Lohrenz, J. C. W.; Kühn, A.; Boche, G. *Tetrahedron* **2000**, *56*, 4109−4115.
(21) Zhao, C.; Wang, D.; Phillips, D. L. *J. Am. Chem. Soc.* **2003**, *125*, 15200−15209.
(22) Meng, F.; Xu, X.; Liu, X.; Zhang, S.; Lu, X. *J. Mol. Struct.: THEOCHEM* **2008**, *858*, 66−71.
(23) Blanchard, E. P.; Simmons, H. E. *J. Am. Chem. Soc.* **1964**, *86*, 1337−1347.
(24) Pratt, L. M.; Ramachandran, B.; Xidos, J. D.; Cramer, C. J.; Truhlar, D. G. *J. Org. Chem.* **2002**, *67*, 7607−7612.
(25) Kottke, T.; Stalke, D. *Angew. Chem., Int. Ed.* **1993**, *32*, 580−582.
(26) Pratt, L. M. *Bull. Chem. Soc. Jpn.* **2009**, *82*, 1107−1125.
(27) Ke, Z.; Zhao, C.; Phillips, D. L. *J. Org. Chem.* **2007**, *72*, 848−860.
(28) Staroscik, J. A.; Rickborn, B. *J. Org. Chem.* **1972**, *37*, 738−740.
(29) Fabisch, B.; Mitchell, T. N. *J. Organomet. Chem.* **1984**, *269*, 219−221.
(30) Oh, C. H.; Park, D. I.; Ryu, J. H.; Cho, J. H.; Han, J. S. *Bull. Korean Chem. Soc.* **2007**, *28*, 322−324.
(31) Wang, L.; Zou, J.-J.; Zhang, X.; Wang, L. *Energy Fuels* **2011**, *25*, 1342−1347.
(32) Li, Y.; Zou, J.-J.; Zhang, X.; Wang, L.; Mi, Z. *Fuel* **2010**, *89*, 2522−2527.
(33) Wang, L.; Zhang, X.; Zou, J.-J.; Han, H.; Li, Y.; Wang, L. *Energy Fuels* **2009**, *23*, 2383−2388.
(34) Zhao, Y.; Truhlar, D. G. *Theor. Chem. Acc.* **2008**, *120*, 215−241.
(35) Eger, W. A.; Zercher, C. K.; Williams, C. M. *J. Org. Chem.* **2010**, *75*, 7322−7331.
(36) Hay, P. J.; Wadt, W. R. *J. Chem. Phys.* **1985**, *82*, 299−310.
(37) Wadt, W. R.; Hay, P. J. *J. Chem. Phys.* **1985**, *82*, 284−298.
(38) Hay, P. J.; Wadt, W. R. *J. Chem. Phys.* **1985**, *82*, 270−283.
(39) Gonzalez, C. S.; Schlegel, H. B. *J. Phys. Chem.* **1990**, *94*, 5523−5527.
(40) Gonzalez, C. S.; Schlegel, H. B. *J. Chem. Phys.* **1989**, *90*, 2154−2161.
(41) Reed, A. E.; Curtiss, L. A.; Weinhold, F. *Chem. Rev.* **1988**, *88*, 899−926.

(42) Reed, A. E.; Weinhold, F.; Curtiss, L. A.; Pochatko, D. J. *J. Chem. Phys.* **1986**, *84*, 5687−5705.
(43) Frisch, M. J.; Trucks, G. W.; Schlegel, H. B.; Scuseria, G. E.; Robb, M. A.; Cheeseman, J. R.; Scalmani, G.; Barone, V.; Mennucci, B.; Petersson, G. A.; Nakatsuji, H.; Caricato, M.; Li, X.; Hratchian, H. P.; Izmaylov, A. F.; Bloino, J.; Zheng, G.; Sonnenberg, J. L.; Hada, M.; Ehara, M.; Toyota, K.; Fukuda, R., Hasegawa, J.; Ishida, M.; Nakajima, T.; Honda, Y.; Kitao, O.; Nakai, H.; Vreven, T.; Montgomery, J. A. Jr.; Peralta, J. E.; Ogliaro, F.; Bearpark, M.; Heyd, J. J.; Brothers, E.; Kudin, K. N.; Staroverov, V. N.; Keith, T.; Kobayashi, R.; Normand, J.; Raghavachari, K.; Rendell, A.; Burant, J. C.; Iyengar, S. S.; Tomasi, J.; Cossi, M.; Rega, N.; Millam, J. M.; Klene, M.; Knox, J. E.; Cross, J. B.; Bakken, V.; Adamo, C.; Jaramillo, J.; Gomperts, R.; Stratmann, R. E.; Yazyev, O.; Austin, A. J.; Cammi, R.; Pomelli, C.; Ochterski, J. W.; Martin, R. L.; Morokuma, K.; Zakrzewski, V. G.; Voth, G. A.; Salvador, P; Dannenberg, J. J.; Dapprich, S.; Daniels, A. D.; Farkas, O.; Foresman, J. B.; Ortiz, J. V.; Cioslowski, J.; Fox, D. J. *Gaussian 09, revision C.01*; Gaussian, Inc., Wallingford, CT, 2010.
(44) Wong, M. W.; Wiberg, K. B.; Frisch, M. *J. Chem. Phys.* **1991**, *95*, 8991−8998.
(45) Wong, M. W.; Frisch, M. J.; Wiberg, K. B. *J. Am. Chem. Soc.* **1991**, *113*, 4776−4782.